

Photon Upconversion

International Edition: DOI: 10.1002/anie.201703012
German Edition: DOI: 10.1002/ange.201703012Confining Excitation Energy in Er³⁺-Sensitized Upconversion Nanocrystals through Tm³⁺-Mediated Transient Energy Trapping

Qiushui Chen, Xiaoji Xie, Bolong Huang, Liangliang Liang, Sanyang Han, Zhigao Yi, Yu Wang, Ying Li, Dianyuan Fan, Ling Huang,* and Xiaogang Liu*

Abstract: A new class of lanthanide-doped upconversion nanoparticles are presented that are without Yb³⁺ or Nd³⁺ sensitizers in the host lattice. In erbium-enriched core-shell NaErF₄:Tm (0.5 mol %)/NaYF₄ nanoparticles, a high degree of energy migration between Er³⁺ ions occurs to suppress the effect of concentration quenching upon surface coating. Unlike the conventional Yb³⁺-Er³⁺ system, the Er³⁺ ion can serve as both the sensitizer and activator to enable an effective upconversion process. Importantly, an appropriate doping of Tm³⁺ has been demonstrated to further enhance upconversion luminescence through energy trapping. This endows the resultant nanoparticles with bright red (about 700-fold enhancement) and near-infrared luminescence that is achievable under multiple excitation wavelengths. This is a fundamental new pathway to mitigate the concentration quenching effect, thus offering a convenient method for red-emitting upconversion nanoprobes for biological applications.

Photon upconversion in lanthanide-doped nanocrystals that converts near-infrared excitation into visible emissions has enabled many promising applications in anti-counterfeiting,^[1] molecular sensing,^[2] bioimaging,^[3] and therapeutics.^[4] However, an appropriate co-doping strategy involving low concentrations of a sensitizer-activator pair (for example, Yb³⁺-Tm³⁺, Yb³⁺-Er³⁺, or Yb³⁺-Ho³⁺) is typically required to construct high-efficiency upconversion nanocrystals.^[5] Notably, doping high concentrations of sensitizers (Yb³⁺ >

20 mol%) or activators (for example, Er³⁺ > 2%) is known to induce severe luminescence quenching through cross-relaxation or the mechanism of energy migration to surface defects.^[6] As a result of this inherent limitation, a relatively low doping level of lanthanide activators is generally implemented.^[7]

A high power density of excitation (ca. 10⁶ W cm⁻²) has been demonstrated to effectively alleviate luminescence concentration quenching in nanoparticles with heavily doped activators (ca. 20% Er³⁺ or ≈ 8% Tm³⁺).^[8] Another general strategy to prevent the concentration quenching is to implement a core-shell design by which the dominant luminescence quenching through energy migration to surface defects can be effectively blocked (Figure 1a).^[9] However,

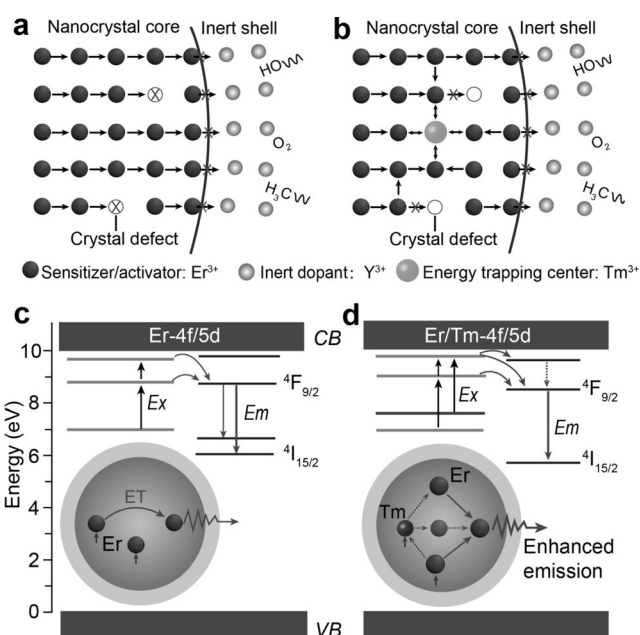


Figure 1. Energy migration in an Er³⁺-based upconversion nanocrystal. a) Typical strategy of preventing energy migration to surface defects and eliminating luminescence quenching in nanocrystals through inert-shell coating. This strategy is not able to mitigate the luminescence quenching caused by energy migration to crystal defects present inside the nanocrystal. b) Proposed mechanism involving the use of a Tm³⁺-mediated trapping center for energy condensation in a core-shell nanocrystal to prevent energy migration over a long distance, resulting in enhanced photon upconversion in the nanocrystal. c) Simplified energy level diagrams and energy transfer process in all Er³⁺-based host sensitization nanocrystals. d) Re-alignment of energy levels of 4f/5d orbitals in upconversion nanocrystals through Tm³⁺/Er³⁺ codoping. The transfer of excitation energy to luminescence centers is boosted by a Tm³⁺-mediated energy trapping process.

[*] Dr. Q. Chen, Dr. Y. Wang, Prof. Y. Li, Prof. D. Fan
-NUS-SZU Collaborative Innovation Center for Optoelectronic Science & Technology, Key Laboratory of Optoelectronic Devices and Systems of Ministry of Education and Guangdong Province College of Optoelectronic Engineering, Shenzhen University Shenzhen 518060 (China)

Prof. X. Xie, Prof. L. Huang
Key Laboratory of Flexible Electronics & Institute of Advanced Materials, Jiangsu National Synergistic Innovation Center for Advanced Materials, Nanjing Tech University Nanjing, 211816 (China)
E-mail: iamlihuang@njtech.edu.cn

Prof. B. Huang
Department of Applied Biology and Chemical Technology
The Hong Kong Polytechnic University
Hung Hom, Kowloon, Hong Kong SAR (China)

Dr. Q. Chen, L. Liang, Dr. S. Han, Z. Yi, Prof. X. Liu
Department of Chemistry, National University of Singapore
Singapore 117543 (Singapore)
E-mail: chmlx@nus.edu.sg

Supporting information and the ORCID identification number(s) for the author(s) of this article can be found under:
<https://doi.org/10.1002/anie.201703012>.

this surface coating method is unable to mitigate the luminescence quenching caused by the energy migration to internal lattice defects.^[10] On the basis of previous findings, we reason that it might be possible to overcome this constraint by introducing a trapping center to confine the excitation energy and minimize the migration-mediated energy loss in the lattice. We realize that an effective energy transfer within a pair of Er^{3+} ions, mediated by impurity doping, is likely to suppress the isotropic migration of excitation energy (Figure 1b).

Through calculations based on density function theory (DFT), we find that Tm^{3+} -doping can lead to a subtle local realignment of the 4f/5d orbitals of Er^{3+} sub-lattice, meaning that all 4f/5d orbitals with spin-up configuration are promoted to energy levels slightly higher than the 4f orbitals with spin-down configuration (Figure 1c,d). The spin-flip-flop is more energetically favorable for the transportation of those excitation energies to Er^{3+} activator through a successive triplet dipole de-excitation.^[11] Thus, we anticipate that the effective harvesting and preservation of excitation energies by Er^{3+} ions for enhanced upconversion luminescence can be facilitated through the use of Tm^{3+} as a transient energy trapping center. Herein we report the synthesis and characterization of $\text{NaErF}_4:\text{Tm}$ (0.5 mol %) $@\text{NaYF}_4$ nanocrystals for host-sensitized upconversion. We demonstrate the possibility of enhancing upconversion luminescence in Er^{3+} -heavily-doped nanocrystals via energy condensation through combined effects of Tm^{3+} -mediated transient energy trapping and inert-shell coating. Our fundamental investigations and theoretical calculations reveal the phenomenon and evidence of Er^{3+} ions acting as both the sensitizer and emitter.

We first prepared $\text{NaErF}_4:\text{Tm}$ (0.5 mol %) core nanocrystals, followed by coating with an inert shell of NaYF_4 via a co-precipitation method according to previous reports.^[12] X-ray powder diffraction studies revealed the hexagonal phase of the as-prepared samples (see Figure S1 in the Supporting Information). A representative low-resolution transmission electron microscopy (TEM) image shows high monodispersity of the resulting particles (Figure 2a). These core and core-shell nanoparticles are 19.7 nm and 28.6 nm in diameter on average (Figure S2, Supporting Information). High-resolution TEM image of an individual core-shell nanocrystal exhibits the lattice fringe of (110) planes with a d -spacing of 0.53 nm, which is in good agreement with that of its hexagonal-phased NaYF_4 counterpart. According to our theoretical calculations, the Er^{3+} ions doped in the as-synthesized nanocrystals are capable of acting as both the sensitizer and emitter, while the Tm^{3+} dopant can serve as the center for energy trapping (Figure 2b; Figure S3 in the Supporting Information). We thereafter measured the luminescence spectra of $\text{NaErF}_4:\text{Tm}$ (0.5 mol %) core and $\text{NaErF}_4:\text{Tm}$ (0.5 mol %) $@\text{NaYF}_4$ core-shell nanocrystals dispersed in cyclohexane solutions (Figure 2c). Surprisingly, we observed that with the coating of an inert shell layer onto the Er^{3+} -based nanoparticle the emission of the particle at 654 nm is significantly enhanced by a factor of 708 times. We also recorded a severe quenching in upconversion luminescence of the core nanocrystals, indicating a high level of energy migration to surface defects. The intensity ratio of red-to-

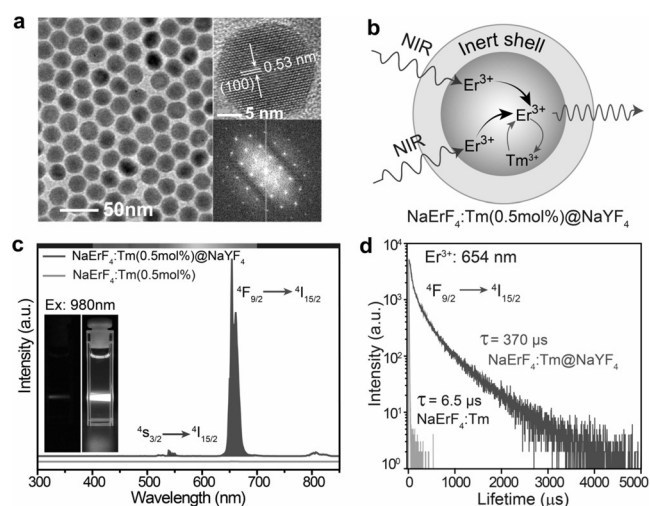


Figure 2. a) Typical low-resolution TEM image (left), high-resolution TEM photograph (upper right), and the corresponding Fourier transform diffraction pattern (lower right) of the as-prepared $\text{NaErF}_4:\text{Tm}$ (0.5 mol %) $@\text{NaYF}_4$ nanoparticles. b) Proposed mechanism involving energy transfer upconversion with Er^{3+} ions acting as both sensitizer and emitter and with Tm^{3+} dopant as energy trapping center. c) Luminescence spectra of $\text{NaErF}_4:\text{Tm}$ (0.5 mol %) core and $\text{NaErF}_4:\text{Tm}$ (0.5 mol %) $@\text{NaYF}_4$ core-shell nanoparticles dispersed in cyclohexane solutions. The data were recorded under 980 nm diode laser excitation, and the emission spectra were compared at 654 nm of Er^{3+} emission. Insets: two typical photographs showing the luminescence of the core (left) and core-shell (right) nanocrystals. d) Corresponding luminescence decay curves of Er^{3+} ions measured at 654 nm for the core and NaYF_4 shell-coated nanocrystals, respectively.

green emission of the as-synthesized core-shell nanoparticles is much larger than that observed in typical $\text{NaYF}_4:\text{Yb/Er}$ (18/2 mol %) nanocrystals. This is true even under a high pumping power density (Figure S4, Supporting Information). To examine the energy migration in Er^{3+} -based core nanocrystals, we further measured their lifetime decay at the $^4\text{F}_{9/2}$ state of Er^{3+} (Figure 2d). A short lifetime of about 6.5 μs from $\text{NaErF}_4:\text{Tm}$ (0.5 mol %) nanocrystals suggests the occurrence of luminescence quenching due to rapid energy migration to lattice defects or surface quenchers. By comparison, the lifetime of Er^{3+} emission from $\text{NaErF}_4:\text{Tm}$ (0.5 mol %) $@\text{NaYF}_4$ nanocrystals was significantly increased to about 370 μs , suggesting the effective suppression of luminescence quenching.

The energy migration through Er^{3+} ions to surface defects is further studied by optical investigation of nanoparticles upon surface passivation. On increasing the inert-shell thickness of NaYF_4 from 0 to 4 nm, we observed a significant enhancement of upconversion luminescence at 654 nm (Figure S5, Supporting Information). We reason that the luminescence quenching induced by cross-relaxation will not dominate in the nanocrystals heavily doped with Er^{3+} ions, because the recovery in excitation energy would occur due to a large spectral overlap between the emission and absorption bands of Er^{3+} ions around 1532 nm (Figure S6, Supporting Information). To examine the concentration quenching effects in the Er^{3+} -sensitized nanocrystal, we measured the emission spectra of $\text{NaYF}_4:\text{Er}@\text{NaYF}_4$ nanoparticles with different amounts of Er^{3+} (20 to 100 mol %) (Figure 3a). Our

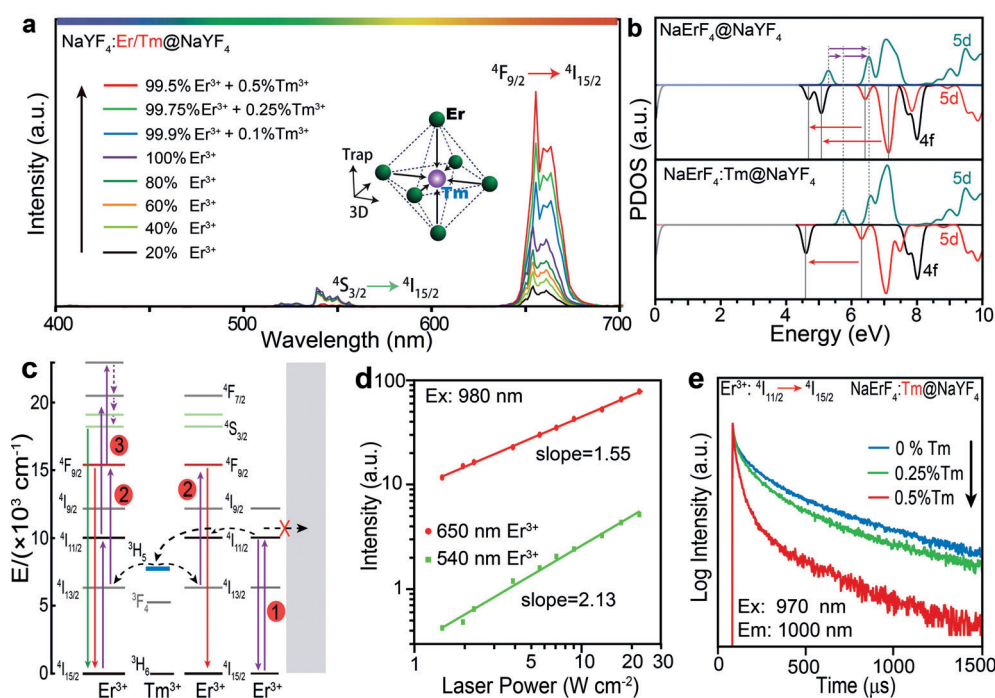


Figure 3. a) Emission spectra of the NaYF₄:Er/Tm@NaYF₄ nanoparticles doped with different Er³⁺ concentration (20, 40, 60, 80, and 100 mol%) and Tm³⁺ concentration (0, 0.1, 0.25, and 0.5 mol%) in the core, showing an increased in emission intensity with increasing dopant content. The spectral comparison of NaErF₄@NaYF₄ nanoparticles with Tm³⁺-doped counterparts shows an additional enhancement in the luminescence emission. Inset: a structural model for Tm³⁺-mediated energy condensation between Er³⁺ ions. b) Projected partial density of states (PDOS) of the transient states given by the NaErF₄ lattice with and without Tm³⁺ dopants. c) Proposed upconversion mechanisms for NaErF₄:Tm (0.5 mol%) nanoparticles under excitation with a 980 nm diode laser. An inert shell is typically coated on the NaErF₄:Tm core to prevent strong energy migration through Er³⁺-Er³⁺ ion pairs to surface defects. The solid purple, dashed black, and solid red (green) arrows represent photon excitation, energy transfer, and radiative emission, respectively. d) Power density dependence of Er³⁺ emission at 654 nm, indicating a two-photon population process for red emission and a three-photon population process for green emission in the NaErF₄:Tm (0.5 mol%)@NaYF₄ nanocrystals under excitation of a 980-nm diode laser. e) The corresponding luminescence lifetimes of Er³⁺ at its ⁴I_{11/2} state in NaErF₄@NaYF₄ nanoparticles doped with various concentrations of Tm³⁺ ions (0, 0.25, and 0.5 mol%). The excitation and emission wavelengths were fixed at 970 nm and 1000 nm, respectively.

data support the idea that the enhancement of upconversion luminescence can be achieved by increasing the Er³⁺ concentration in the particle core without concerning the concentration quenching effect. It should be noted that this phenomenon was also reported in a recent investigation led by Almutairi and co-workers.^[13] Accordingly, the red-to-green ratio of the peaks at 654 nm and 540 nm increases with increasing Er³⁺ content (Figure S7, Supporting Information).

It is important to note that a further codoping of Tm³⁺ ions to the Er³⁺-based host lead to an added enhancement in emission intensity (Figure 3a). This investigation strongly validates our proposed concept of energy condensation through Tm³⁺-mediated transient energy trapping, which prevents distant energy migration and thereby minimizes the energy loss at defective lattice sites. To gain fundamental insights into the mechanism underlying the energy trapping by Tm³⁺ ions, we carried out DFT calculations to study projected partial density of states (PDOS) at the transient states given by the NaErF₄ lattices with and without Tm³⁺ doping (Figure 3b). The results showed that the Tm³⁺ doping causes a re-alignment in the energy levels of lanthanide ions

(Figure S8, Supporting Information). Notably, the Tm³⁺-codoped system enables a relatively small reduction in energy interval and allows the excited electrons to be accumulated in favor of excited-state population. This process minimizes energy migration to particle surface and promotes trapping of the excitation energy. Moreover, through the Tm³⁺ codoping strategy the 4f/5d orbitals of Er³⁺ can be raised to higher energy levels, facilitating the energy transfer from an excited Er³⁺ ion to a neighboring Er³⁺ activator ion residing at the ground state. As a result, an enhanced upconversion emission at 654 nm was experimentally observed.

For illumination of the energy transfer mechanism, let us consider the case of Er³⁺ ions with dual functions for energy harvesting and emission in Er³⁺-based nanocrystals (Figure 3c). Indeed, the population of one 980 nm photon at the ⁴I_{11/2} state of a given Er³⁺ ion can be realized by direct excitation or through energy transfer from an adjacent Er³⁺ ion. We found that an optimal doping of Tm³⁺ (0.5 mol%) into the Er³⁺-based host leads to the trapping of the populated energy at the ³H₅ state of Tm³⁺ (Figure S9, Supporting Information). Subsequently, a back-energy-transfer process from the ³H₅ state of Tm³⁺ to the ⁴I_{13/2} state of Er³⁺ takes place, followed by energy pumping with a second 980-nm photon to the ⁴F_{9/2} state of Er³⁺. Consequently, a red emission at 654 nm dominates the upconversion process.

Our proposed mechanism was further confirmed by power density-dependent luminescence studies, which were in accord with the above-mentioned energy transfer progress (Figure 3d). Notably, the three-photon population process for green emission is strongly suppressed, because the distance between Er³⁺ ions shortens with increasing concentrations. This may also lead to an increased rate of energy migration as confirmed by lifetime measurements of Er³⁺ emission at its ⁴F_{9/2} state (Figure S10, Supporting Information). Furthermore, we investigated time-resolved population at the ⁴I_{11/2} state of Er³⁺. We observed that on increasing Tm³⁺ dopant concentration, the depopulation at the ⁴I_{11/2} state of Er³⁺ is accelerated by Tm³⁺-mediated trapping through energy

transfer (Figure 3e). This evidence clearly supports the role of Tm^{3+} ions in trapping energies from the $^4\text{I}_{11/2}$ state of Er^{3+} . The Tm^{3+} -mediated transient energy transfer was further confirmed by spectral comparison under the excitation of 1532 nm (Figure S11, Supporting Information). Taken together, these results unambiguously suggest that the Tm^{3+} -mediated energy condensation is responsible for minimized loss of excitation energies and thus enhanced luminescence intensity.

The construction of Er^{3+} -based host sensitization upconversion nanocrystals offers a unique ability to generate red emission. The quantum yield of Er^{3+} -sensitized upconversion nanocrystals is comparable to conventional Yb^{3+} -sensitized upconversion nanoparticles under excitation with a 980-nm diode laser (Table S1, Supporting Information). Meanwhile, we observed that the upconversion luminescence of Er^{3+} -sensitized nanoparticles is stronger than cubic-phased $\text{KMnF}_3\text{:Yb/Er}$ and $\text{NaYF}_4\text{:Yb/Er}$ nanoparticles, while comparable to $\text{Yb}^{3+}/\text{Tm}^{3+}$ -codoped hexagonal-phased nanoparticles but weaker than $\text{Yb}^{3+}/\text{Er}^{3+}$ -based hexagonal core-shell nanoparticles (Figure S12, Supporting Information). Although the absorption cross-section of Er^{3+} at 980 nm is lower than that of Yb^{3+} , the amount of luminescence centers in $\text{NaErF}_4\text{:Tm}(0.5\%)\text{@NaYF}_4$ nanocrystals is much larger than that available in $\text{Yb}^{3+}/\text{Er}^{3+}$ -codoped counterparts. Different from Yb^{3+} - and Nd^{3+} -based nanocrystals excitable only at 980 and 808 nm, respectively, Er^{3+} -based nanocrystals can be efficiently excited by three different wavelengths: 808, 980, and 1532 nm (Figure 4a). Such being the case, our Er^{3+} -based upconversion nanoprobe permits in vivo imaging using three different laser sources for excitations (Figure 4b). The precise management of excitation and emission in a broad optical

window will enable optimal consideration of detection sensitivity, light penetration, and photothermal effects in the context of in vivo imaging (Figure 4c).^[14]

In conclusion, we have presented a new class of hexagonal-phased $\text{NaErF}_4\text{:Tm}(0.5\text{ mol \%})\text{@NaYF}_4$ nanocrystals with bright red upconversion luminescence through Er^{3+} -based host sensitization. Our mechanistic investigation reveals that the luminescence quenching in the Er^{3+} -based nanocrystals is mainly dominated by rapid energy migration, rather than cross-relaxation often observed in conventional $\text{Yb}^{3+}/\text{Er}^{3+}$ -codoped nanocrystals. Encouraged by this finding, we demonstrate that the concentration-induced quenching of luminescence in the nanocrystals under study can be largely suppressed by employing a core-shell structure. More importantly, through the use of Tm^{3+} dopants we have devised a new strategy to minimize energy losses at defective crystal sites. The effect of Tm^{3+} ions for trapping excitation energies is harnessed to maximally minimize the luminescence quenching effects by preventing distant energy migration in the host lattice. This study may open up new avenues of research on the development of multi-wavelength-excitable upconversion nanocrystals suitable for particular biomedical or security applications.

Acknowledgements

This work was supported by the Singapore Ministry of Education (Grant R143000627112, R143000642112), Agency for Science, Technology and Research (A*STAR) under the contracts of 122-PSE-0014 and 1231AFG028 (Singapore), Singapore National Research Foundation, the National Natural Science Foundation of China (Grant 6157030930, 61490713), the Science and Technology Planning Project of Guangdong Province (Grant 2016B050501005), and the Educational Commission of Guangdong Province (Grant 2016KCXTD006). We thank Dr. R. Deng and Dr. J. Peng for helpful discussion.

Conflict of interest

The authors declare no conflict of interest.

Keywords: energy migration · Er^{3+} sensitizers · optical imaging · transient energy trapping · upconversion nanocrystals

How to cite: *Angew. Chem. Int. Ed.* **2017**, *56*, 7605–7609
Angew. Chem. **2017**, *129*, 7713–7717

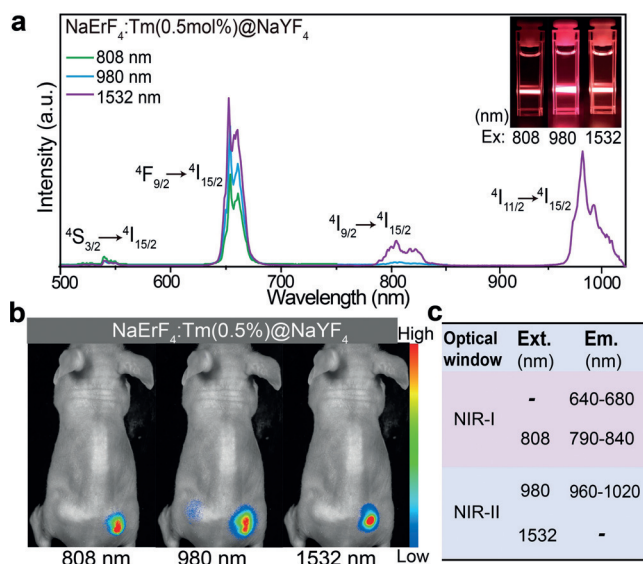


Figure 4. a) Emission spectra recorded for $\text{NaErF}_4\text{:Tm}(0.5\text{ mol \%})\text{@NaYF}_4$ nanoparticles when illuminated at 808, 980, and 1532 nm. Insets: corresponding photographs of the colloidal solutions irradiated under three different lasers. b) In vivo optical imaging using silica-coated $\text{NaErF}_4\text{:Tm}(0.5\text{ mol \%})\text{@NaYF}_4$ nanoparticles, recorded under excitation at 808, 980, and 1532 nm. c) The compiled luminescence profiles for the as-synthesized nanocrystals.

- Chen, *Angew. Chem. Int. Ed.* **2015**, *54*, 7915–7919; *Angew. Chem.* **2015**, *127*, 8026–8030; e) S. H. Nam, Y. M. Bae, Y. I. Park, J. H. Kim, H. M. Kim, J. S. Choi, K. T. Lee, T. Hyeon, Y. D. Suh, *Angew. Chem. Int. Ed.* **2011**, *50*, 6093–6097; *Angew. Chem.* **2011**, *123*, 6217–6221; f) Q. Su, W. Feng, D. Yang, F. Li, *Acc. Chem. Res.* **2017**, *50*, 32–40.
- [3] a) Y. F. Wang, G. Y. Liu, L. D. Sun, J. W. Xiao, J. C. Zhou, C. H. Yan, *ACS Nano* **2013**, *7*, 7200–7206; b) X. Xie, N. Gao, R. Deng, Q. Sun, Q. H. Xu, X. Liu, *J. Am. Chem. Soc.* **2013**, *135*, 12608–12611; c) J. C. Boyer, M. P. Manseau, J. I. Murray, F. C. van Veggel, *Langmuir* **2010**, *26*, 1157–1164; d) Y. I. Park, K. T. Lee, Y. D. Suh, T. Hyeon, *Chem. Soc. Rev.* **2015**, *44*, 1302–1317; e) R. Wang, X. Li, L. Zhou, F. Zhang, *Angew. Chem. Int. Ed.* **2014**, *53*, 12086–12090; *Angew. Chem.* **2014**, *126*, 12282–12286.
- [4] a) Y. Liu, D. Tu, H. Zhu, X. Chen, *Chem. Soc. Rev.* **2013**, *42*, 6924–6958; b) Y. Zhang, L. Huang, Z. Li, G. Ma, Y. Zhou, G. Han, *ACS Nano* **2016**, *10*, 3881–3885; c) M. H. Chan, C. W. Chen, I. J. Lee, Y. C. Chan, D. Tu, M. Hsiao, C. H. Chen, X. Chen, R. S. Liu, *Inorg. Chem.* **2016**, *55*, 10267–10277; d) A. Punjabi, X. Wu, A. Tokatli-Apollon, M. El-Rifai, H. Lee, Y. Zhang, C. Wang, Z. Liu, E. M. Chan, C. Duan, G. Han, *ACS Nano* **2014**, *8*, 10621–10630; e) J. Xiang, L. Xu, H. Gong, W. Zhu, C. Wang, J. Xu, L. Feng, L. Cheng, R. Peng, Z. Liu, *ACS Nano* **2015**, *9*, 6401–6411; f) D. Yang, P. Ma, Z. Hou, Z. Cheng, C. Li, J. Lin, *Chem. Soc. Rev.* **2015**, *44*, 1416–1448; g) X. Zhu, W. Feng, J. Chang, Y. W. Tan, J. Li, M. Chen, Y. Sun, F. Li, *Nat. Commun.* **2016**, *7*, 10437; h) S. Gai, C. Li, P. Yang, J. Lin, *Chem. Rev.* **2014**, *114*, 2343–2389; i) W. Fan, W. Bu, B. Shen, Q. He, Z. Cui, Y. Liu, X. Zheng, K. Zhao, J. Shi, *Adv. Mater.* **2015**, *27*, 4155–4161; j) J. Liu, Y. Liu, W. Bu, J. Bu, Y. Sun, J. Du, J. Shi, *J. Am. Chem. Soc.* **2014**, *136*, 9701–9709.
- [5] a) F. Auzel, *Chem. Rev.* **2004**, *104*, 139–173; b) J. Hao, Y. Zhang, X. Wei, *Angew. Chem. Int. Ed.* **2011**, *50*, 6876–6880; *Angew. Chem.* **2011**, *123*, 7008–7012; c) J. Shen, G. Chen, A.-M. Vu, W. Fan, O. S. Bilsel, C.-C. Chang, G. Han, *Adv. Opt. Mater.* **2013**, *1*, 644–650; d) T. V. Esipova, X. Ye, J. E. Collins, S. Sakadzic, E. T. Mandeville, C. B. Murray, S. A. Vinogradov, *Proc. Natl. Acad. Sci. USA* **2012**, *109*, 20826–20831; e) X. Li, Z. Guo, T. Zhao, Y. Lu, L. Zhou, D. Zhao, F. Zhang, *Angew. Chem. Int. Ed.* **2016**, *55*, 2464–2469; *Angew. Chem.* **2016**, *128*, 2510–2515; f) P. Rodríguez-Sevilla, Y. Zhang, N. de Sousa, M. I. Marqués, F. Sanz-Rodríguez, D. Jaque, X. Liu, P. Haro-González, *Nano Lett.* **2016**, *16*, 8005–8014; g) H. Schäfer, P. Ptacek, H. Eickmeier, M. Haase, *Adv. Funct. Mater.* **2009**, *19*, 3091–3097.
- [6] a) M. Haase, H. Schäfer, *Angew. Chem. Int. Ed.* **2011**, *50*, 5808–5829; *Angew. Chem.* **2011**, *123*, 5928–5950; b) Y. Liu, Y. Lu, X. Yang, X. Zheng, S. Wen, F. Wang, X. Vidal, J. Zhao, D. Liu, Z. Zhou, C. Ma, J. Zhou, J. A. Piper, P. Xi, D. Jin, *Nature* **2017**, *543*, 229–233; c) S. Han, R. Deng, X. Xie, X. Liu, *Angew. Chem. Int. Ed.* **2014**, *53*, 11702–11715; *Angew. Chem.* **2014**, *126*, 11892–11906; d) Y. Lu, J. Zhao, R. Zhang, Y. Liu, D. Liu, E. M. Goldys, X. Yang, P. Xi, A. Sunna, J. Lu, Y. Shi, R. C. Leif, Y. Huo, J. Shen, J. A. Piper, J. P. Robinson, D. Jin, *Nat. Photon.* **2014**, *8*, 32–36; e) F. Vetrone, R. Naccache, V. Mahalingam, C. G. Morgan, J. A. Capobianco, *Adv. Funct. Mater.* **2009**, *19*, 2924–2929; f) H. Wang, W. Lu, T. Zeng, Z. Yi, L. Rao, H. Liu, S. Zeng, *Nanoscale* **2014**, *6*, 2855–2860; g) H. Wang, Z. Yi, L. Rao, H. Liu, S. Zeng, *J. Mater. Chem. C* **2013**, *1*, 5520–5526.
- [7] a) E. M. Chan, D. J. Gargas, P. J. Schuck, D. J. Milliron, *J. Phys. Chem. B* **2012**, *116*, 10561–10570; b) S. Han, X. Qin, Z. An, Y. Zhu, L. Liang, Y. Han, W. Huang, X. Liu, *Nat. Commun.* **2016**, *7*, 13059; c) E. M. Chan, G. Han, J. D. Goldberg, D. J. Gargas, A. D. Ostrowski, P. J. Schuck, B. E. Cohen, D. J. Milliron, *Nano Lett.* **2012**, *12*, 3839–3845; d) G. Chen, T. Y. Ohulchanskyy, A. Kachynski, H. Agren, P. N. Prasad, *ACS Nano* **2011**, *5*, 4981–4986; e) P. Chen, M. Song, E. Wu, B. Wu, J. Zhou, H. Zeng, X. Liu, J. Qiu, *Nanoscale* **2015**, *7*, 6462–6466; f) Z. Hou, K. Deng, C. Li, X. Deng, H. Lian, Z. Cheng, D. Jin, J. Lin, *Biomaterials* **2016**, *101*, 32–46; g) L. L. Li, Y. Lu, *J. Am. Chem. Soc.* **2015**, *137*, 5272–5275; h) P. Rodríguez-Sevilla, Y. Zhang, P. Haro-González, F. Sanz-Rodríguez, F. Jaque, J. G. Solé, X. Liu, D. Jaque, *Adv. Mater.* **2016**, *28*, 2421–2426; i) A. Speghini, F. Piccinelli, M. Bettinelli, *Opt. Mater.* **2011**, *33*, 247–257.
- [8] a) D. J. Gargas, E. M. Chan, A. D. Ostrowski, S. Aloni, M. V. Altoe, E. S. Barnard, B. Sanii, J. J. Urban, D. J. Milliron, B. E. Cohen, P. J. Schuck, *Nat. Nanotechnol.* **2014**, *9*, 300–305; b) J. Zhao, D. Jin, E. P. Scharfner, Y. Lu, Y. Liu, A. V. Zvyagin, L. Zhang, J. M. Dawes, P. Xi, J. A. Piper, E. M. Goldys, T. M. Monro, *Nat. Nanotechnol.* **2013**, *8*, 729–734; c) J. Zhou, G. Chen, Y. Zhu, L. Huo, W. Mao, D. Zou, X. Sun, E. Wu, H. Zeng, J. Zhang, *J. Mater. Chem. C* **2015**, *3*, 364–369.
- [9] a) Q. Su, S. Han, X. Xie, H. Zhu, H. Chen, C. K. Chen, R. S. Liu, X. Chen, F. Wang, X. Liu, *J. Am. Chem. Soc.* **2012**, *134*, 20849–20857; b) G. Chen, H. Agren, T. Y. Ohulchanskyy, P. N. Prasad, *Chem. Soc. Rev.* **2015**, *44*, 1680–1713; c) H. Dong, L. D. Sun, Y. F. Wang, J. Ke, R. Si, J. W. Xiao, G. M. Lyu, S. Shi, C. H. Yan, J. Am. Chem. Soc. **2015**, *137*, 6569–6576; d) H. Dong, L. D. Sun, C. H. Yan, *Chem. Soc. Rev.* **2015**, *44*, 1608–1634; e) W. Shao, G. Chen, A. Kuzmin, H. L. Kutscher, A. Pliss, T. Y. Ohulchanskyy, P. N. Prasad, *J. Am. Chem. Soc.* **2016**, *138*, 16192–16195; f) J. Wang, F. Wang, C. Wang, Z. Liu, X. Liu, *Angew. Chem. Int. Ed.* **2011**, *50*, 10369–10372; *Angew. Chem.* **2011**, *123*, 10553–10556; g) B. Chen, Y. Liu, Y. Xiao, X. Chen, Y. Li, M. Li, X. Qiao, X. Fan, F. Wang, *J. Phys. Chem. Lett.* **2016**, *7*, 4916–4921; h) X. Chen, L. Jin, W. Kong, T. Sun, W. Zhang, X. Liu, J. Fan, S. F. Yu, F. Wang, *Nat. Commun.* **2016**, *7*, 10304.
- [10] a) F. Wang, R. Deng, J. Wang, Q. Wang, Y. Han, H. Zhu, X. Chen, X. Liu, *Nat. Mater.* **2011**, *10*, 968–973; b) J. Wang, R. Deng, M. A. MacDonald, B. Chen, J. Yuan, F. Wang, D. Chi, T. S. Hor, P. Zhang, G. Liu, Y. Han, X. Liu, *Nat. Mater.* **2014**, *13*, 157–162.
- [11] a) P. A. Tanner, *Lanthanide luminescence in solids*. In: *Lanthanide Luminescence*, Springer, Berlin, Heidelberg, **2010**, pp. 183–233; b) B. Huang, *Phys. Chem. Chem. Phys.* **2016**, *18*, 13564–13582.
- [12] a) S. Han, A. Samanta, X. Xie, L. Huang, J. Peng, S. J. Park, D. B. L. Teh, Y. Choi, Y.-T. Chang, A. H. All, Y. Yang, B. Xing, X. Liu, *Adv. Mater.* **2017**, <https://doi.org/10.1002/adma.201700244>; b) C. D. Brites, X. Xie, M. L. Debasu, X. Qin, R. Chen, W. Huang, J. Rocha, X. Liu, L. D. Carlos, *Nat. Nanotechnol.* **2016**, *11*, 851–856.
- [13] N. J. Johnson, S. He, S. Diao, E. M. Chan, H. Dai, A. Almutairi, *J. Am. Chem. Soc.* **2017**, *139*, 3275–3282.
- [14] a) G. Hong, A. L. Antaris, H. Dai, *Nat. Biomed. Eng.* **2017**, *1*, 0010; b) L. Liang, X. Xie, D. T. Loong, A. H. All, L. Huang, X. Liu, *Chem. Eur. J.* **2016**, *22*, 10801–10807.

Manuscript received: March 23, 2017

Accepted manuscript online: May 4, 2017

Version of record online: May 24, 2017